Supplementary Information

Chemerin attenuates acute kidney injury by inhibiting ferroptosis via the AMPK/NRF2/SLC7A11 axis

Yidan Ma[a,b,#], Shengnan Fei[a,b,#], Xu Chen[a], Yuanyuan Gui[a,b], Bing Zhou[a,b], Tianya Xiang[a,b], Jianhang Liu[a], Kun Yue[a,b], Qingxin Li[a,b], Wei Jiang[c], Cheng Sun[d], Xinzhong Huang[a,*]

[a] Department of Nephrology, Affiliated Hospital of Nantong University, 20 Xisi Road, Nantong, Jiangsu, 226001, China.

[b] Medical School of Nantong University, Nantong, Jiangsu, 226001, China.

[c] Department of Emergency Medicine, Affiliated Hospital of Nantong University, Nantong, Jiangsu, 226001, China.

[d] Key Laboratory of Neuroregeneration of Jiangsu and Ministry of Education, NMPA Key Laboratory of Research and Evaluation of Tissue Engineering Technology Products, School of Medicine, Nantong University, Nantong, Jiangsu, 226001, China.

Supplementary Fig. 1

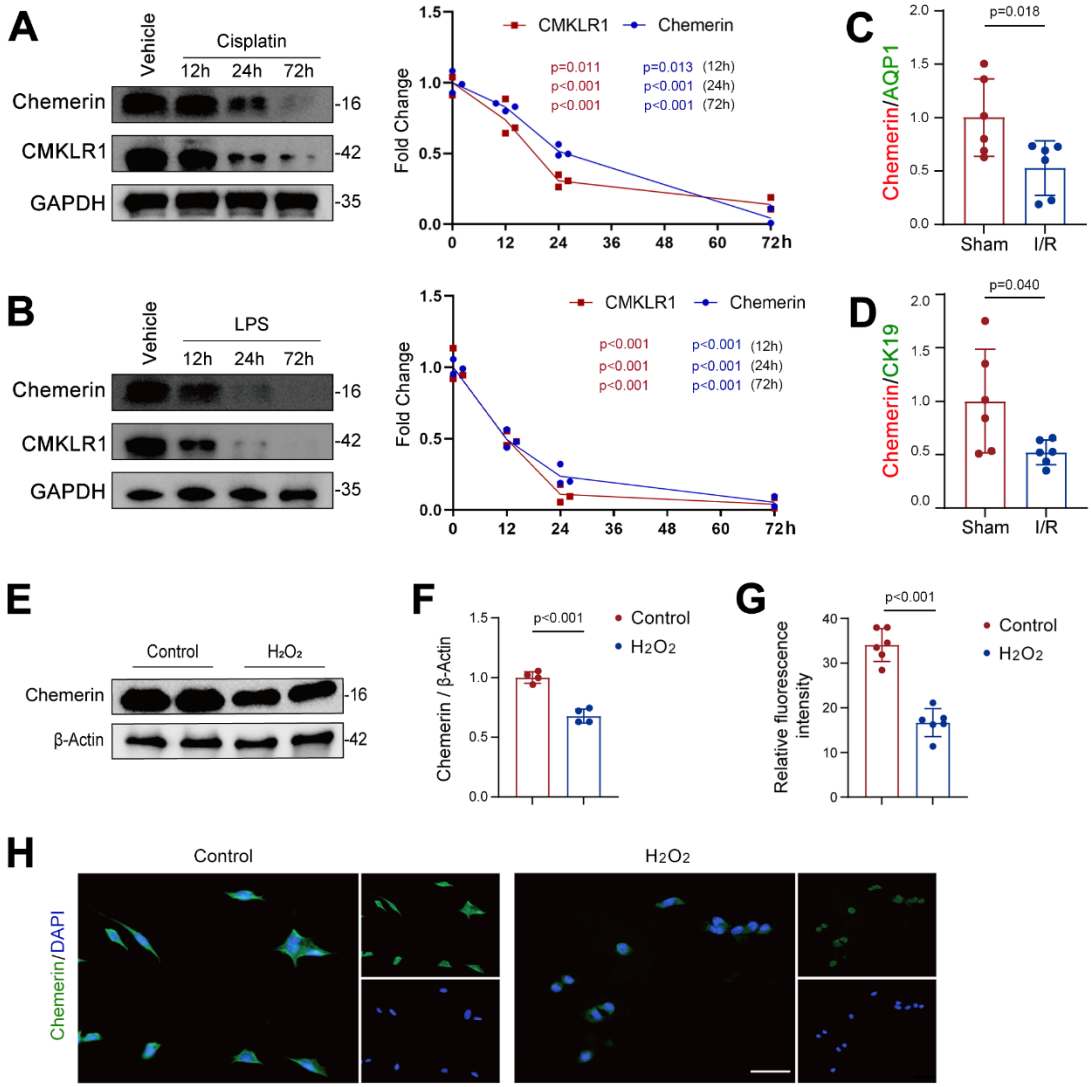

Supplementary Figure 1. Chemerin and its receptor CMKLR1 decreased in the kidneys of AKI model mice and nephropathy patients. (**A-B**) Chemerin and CMKLR1 decreased in the kidneys of Cisplatin- or LPS-treated mice. Mice were treated with Cisplatin (**A**) or LPS (**B**), and kidneys were collected at different time points as indicated for measuring the protein levels of chemerin and CMKLR1. Protein levels were analyzed by western blot, with GAPDH as a loading control. n = 3 (independent experiments). (**C-D**) Chemerin levels with normalization to AQP1 or CK19. (**E**) H_2O_2 treatment reduced chemerin expression in TCMK-1 cells. Cells treated with 100 μM H_2O_2 for 24 h. Protein expression was analyzed by western blot, with β-Actin used as a loading control. n = 3 (independent experiments). (**F**) Quantified data for chemerin from the western blots shown in (**E**). (**G**) Representative immunofluorescence images showing chemerin (green) expression in TCMK-1 cells treated with or without H_2O_2. DAPI was used to

stain the nuclei. Scale bar = 50 μm. n = 6 (independent experiments). (**H**) Quantified data for chemerin staining as shown in (**G**). Data are presented as the mean ± SD, * $p < 0.05$ and *** $p < 0.001$, by one-way ANOVA with Tukey's multiple comparison test.

Supplementary Fig. 2

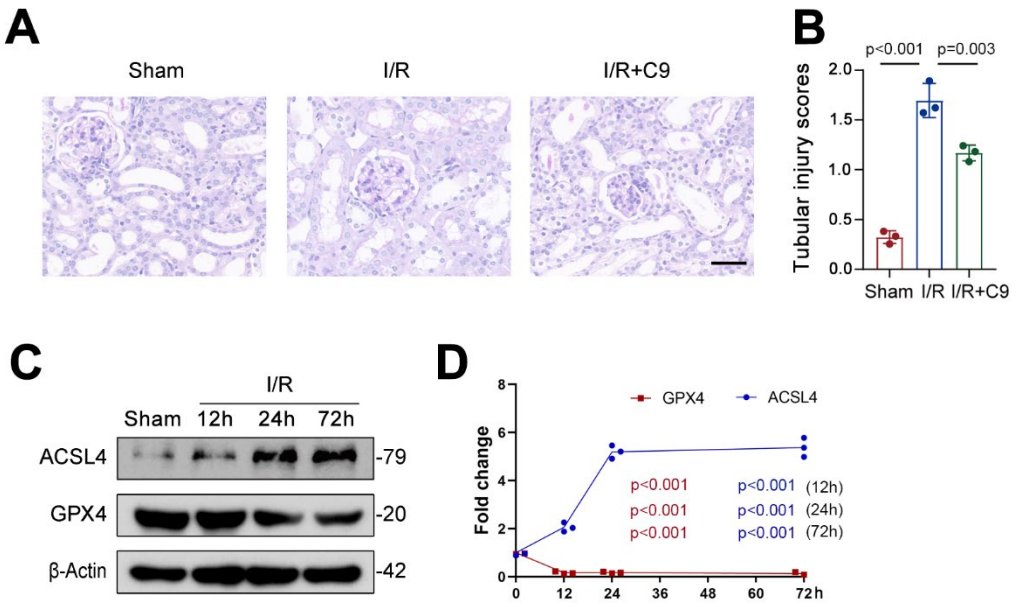

Supplementary Figure 2. C9 treatment alleviates renal injury in I/R model mice and ferroptosis is involved in renal injury induced by I/R. (**A**) Representative periodic acid-Schiff (PAS) staining images of the kidneys. Scale bar = 50 μm. (**B**) Quantified tubular injury scores from the PAS staining shown in (**A**). n = 3 mice/group. (**C**) ACSL4 and GPX4 expression in the kidneys of I/R model mice. Protein levels were analyzed by western blot, with β-Actin used as a loading control. n = 3 (independent experiments). (**D**) Quantified ACSL4 and GPX4 levels based on the western blots in (**C**). Data are presented as the mean ± SD. ** $p < 0.01$ and *** $p < 0.001$, by one-way ANOVA with Tukey's multiple comparison test.

Supplementary Fig. 3

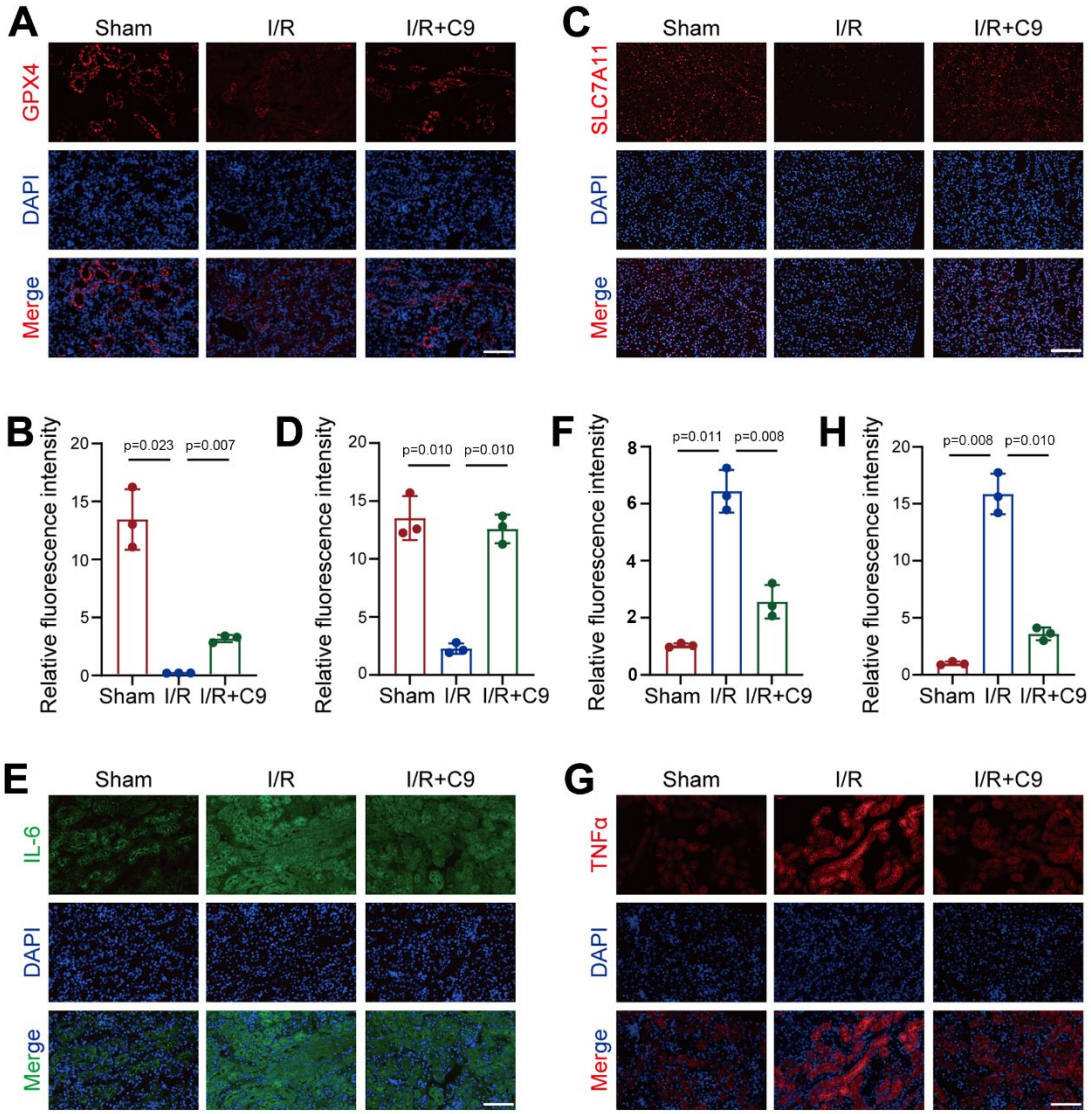

Supplementary Figure 3. Effects of C9 on the expression of IL-6, TNFα, GPX4, and SLC7A11 in the kidneys of I/R model mice. (**A-G**) Representative immunofluorescence images showing GPX4 (**A**), SLC7A11 (**C**), IL-6 (**E**), and TNFα (**G**) expression in the kidneys. Quantified data for each marker are shown in (**B**), (**D**), (**F**), and (**H**), respectively. DAPI was used to stain the nuclei. n = 3 mice/group. Scale bar = 50 μm. Data are presented as the mean ± SD. * $p < 0.05$ and ** $p < 0.01$, by one-way ANOVA with Tukey's multiple comparison test.

Supplementary Fig. 4

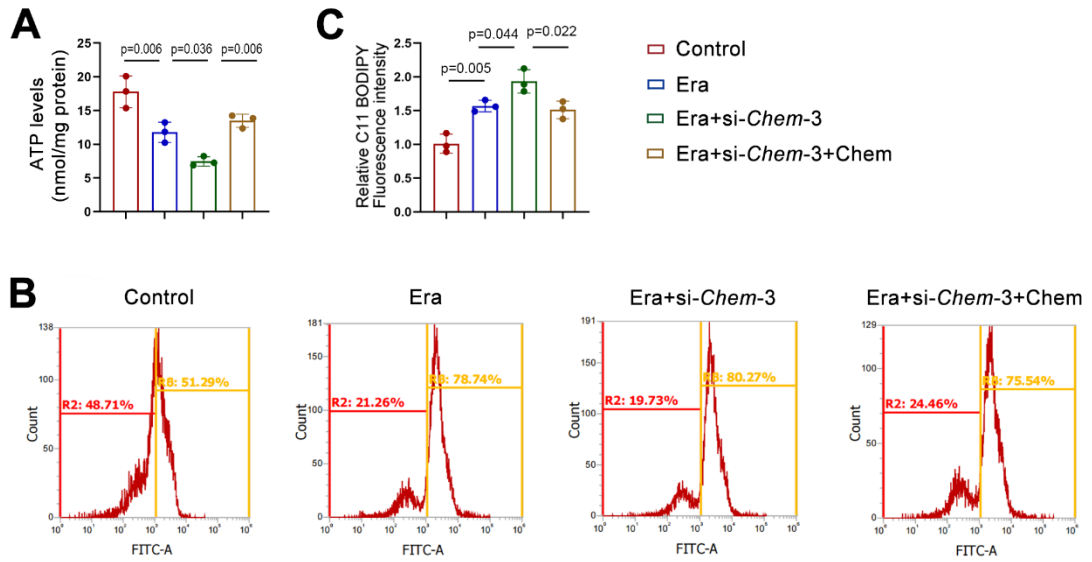

Supplementary Figure 4. Chemerin knockdown aggravates ATP decline and lipid peroxidation induced by erastin. (**A**) Chemerin knockdown decreases intracellular ATP levels in erastin-treated cells. n = 3 (independent experiments). TCMK-1 cells were transfected with si-*Chem*-3. Forty-eight hours post-transfection, cells were treated with recombinant chemerin (20 ng/ml) and erastin (Era, 5 μM) for additional 24 h. (**B**) Chemerin knockdown induces lipid peroxidation in erastin-treated cells. Oxidized lipids were captured using C11 BODIPY and measured by flow cytometry. Cell treatments were described in (**A**). n = 3 (independent experiments). (**C**) Quantified data for lipid peroxidation shown in (**B**). Data are presented as the mean ± SD. * $p < 0.05$ and ** $p < 0.01$, by one-way ANOVA with Tukey's multiple comparison test.

Supplementary Fig. 5

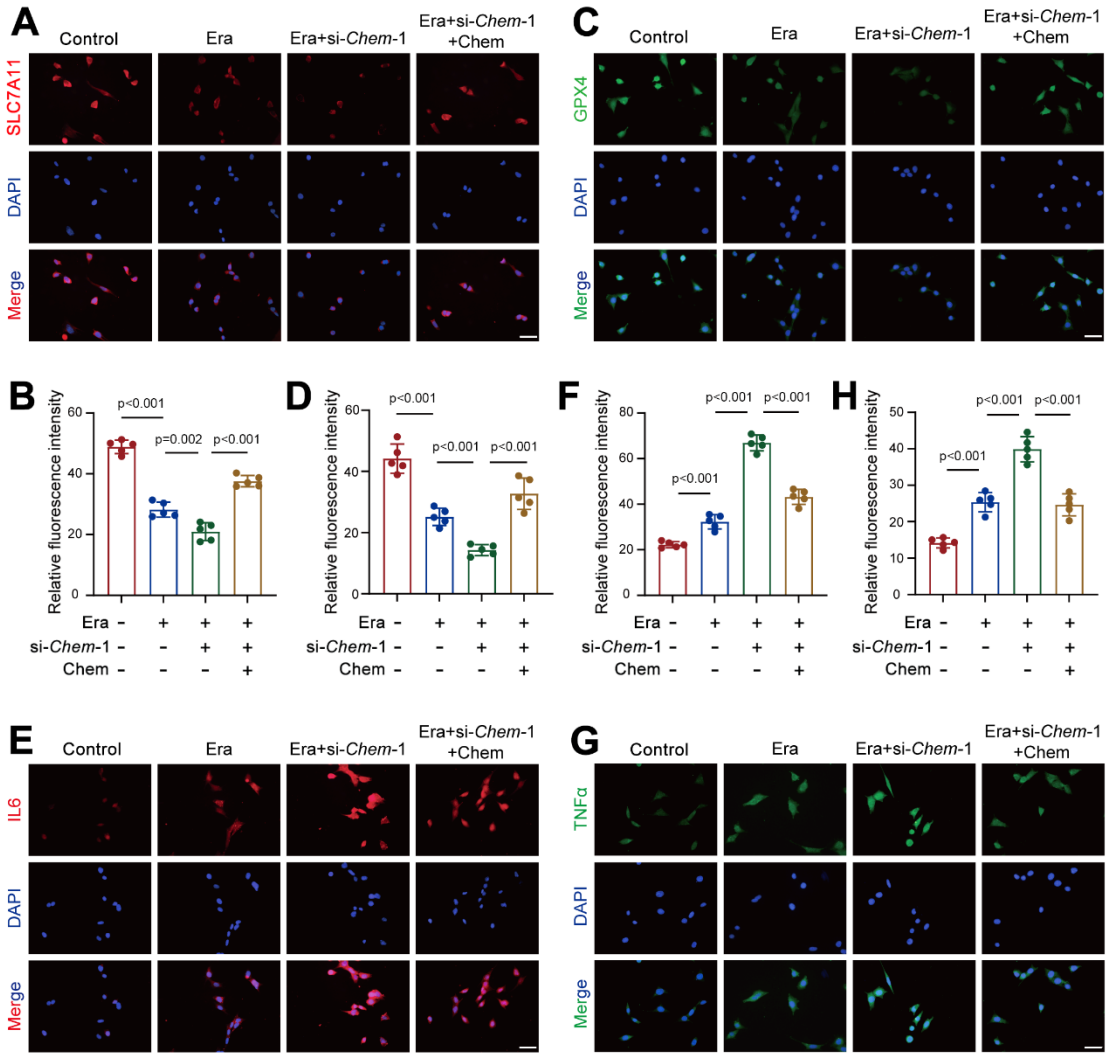

Supplementary Figure 5. Effects of chemerin knockdown on the expression of SLC7A11, GPX4, IL-6, and TNFα in erastin-treated cells. (**A-H**) Representative immunofluorescence staining images for SLC7A11 (**A**), GPX4 (**C**), IL-6 (**E**), and TNFα (**G**) in TCMK-1 cells. The corresponding relative immunofluorescence intensities are shown in (**B**), (**D**), (**F**) and (**H**), respectively. Cells were transfected with siRNA targeting chemerin gene (si-*Chem*). Forty-eight hours post-transfection, cells were treated with recombinant chemerin (20 ng/ml) and erastin (Era, 5 μM) for additional 24 h. n = 5 (independent experiments). Scale bar = 50 μm. Data are presented as the mean ± SD. ** $p < 0.01$ and *** $p < 0.001$, by one-way ANOVA with Tukey's multiple comparison test.

Supplementary Fig. 6

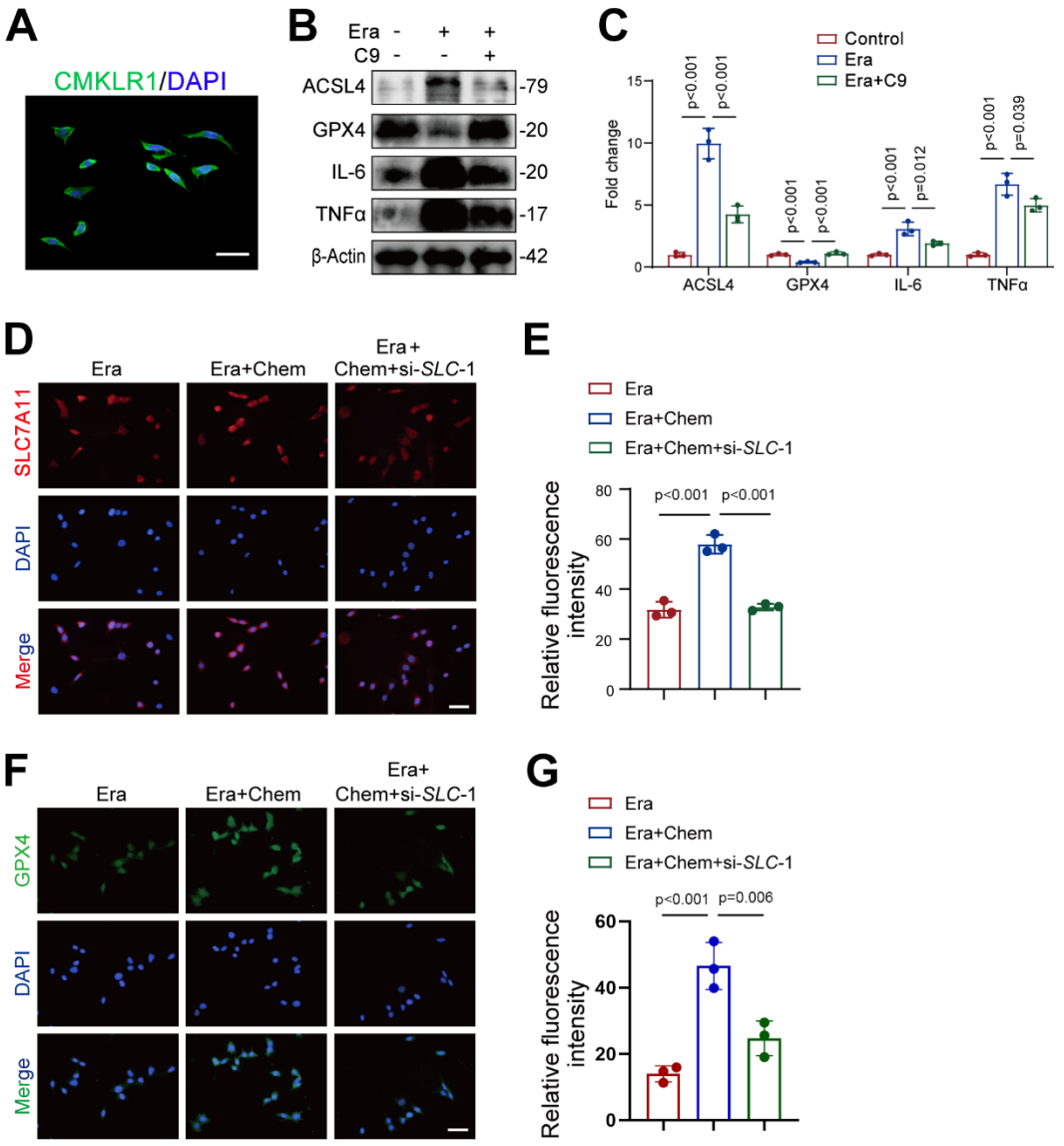

Supplementary Figure 6. SLC7A11 knockdown abolishes the increases in SLC7A11 and GPX4 induced by chemerin in erastin-treated cells. (**A**) TCMK-1 cell expresses CMKLR1. Immunofluorescence was used to examine CMKLR1 expression (green). DAPI (blue) was used to stain the nuclei. Scale bar = 50 μm. (**B**) Chemerin-9 (C9) attenuates erastin-induced changes in ACSL4, GPX4, IL-6 and TNFα, in TCMK-1 cells. Cells were treated with C9 (20 ng/ml) and erastin (Era, 5 μM) for 24 h. Protein expression was analyzed by western blot, with β-Actin used as a loading control. n = 3 (independent experiments). (**C**) Quantified data for the western blots shown in (**B**). (**D-G**) Representative immunofluorescence staining images for SLC7A11 (**D**) and GPX4 (**F**) in TCMK-1 cells. Relative fluorescence intensities are shown in (**E**) and (**G**), respectively. TCMK-1 cells were transfected with si-*SLC*-1 for 48 h, then treated with erastin

(Era, 5 μM) and the recombinant chemerin (20 ng/ml) for an additional 24 h. n = 3 (independent experiments). Scale bar = 50 μm. Data are presented as the mean ± SD. * $p < 0.05$, *** $p < 0.001$, by one-way ANOVA with Tukey's multiple comparison test.

Supplementary Fig. 7

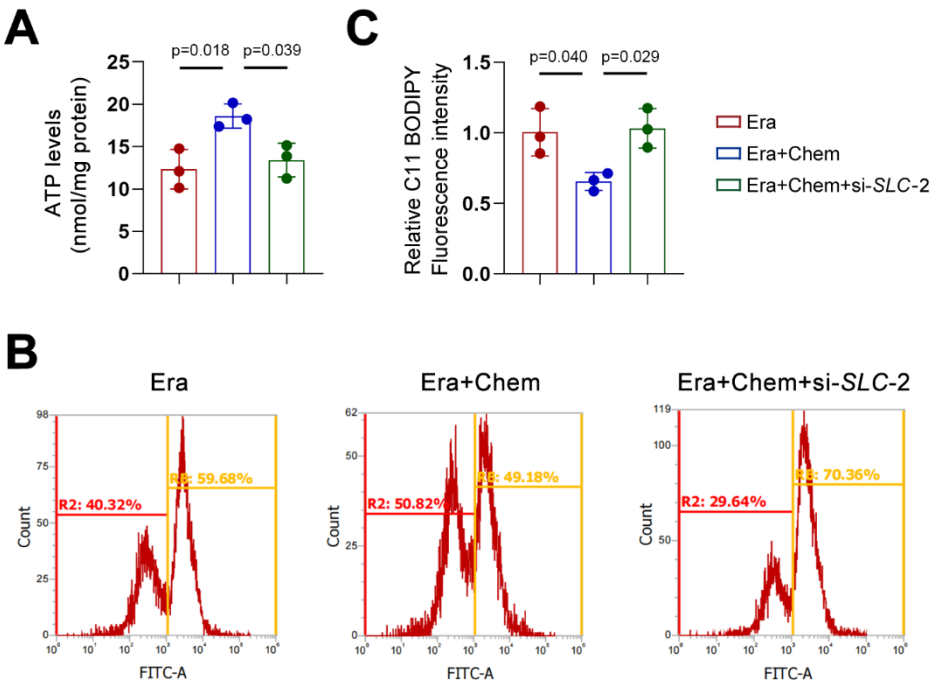

Supplementary Figure 7. SLC7A11 knockdown reverses the improved ATP levels and lipid peroxidation induced by chemerin in erastin-treated cells. TCMK-1 cells were transfected with si-*SLC*-2 for 48 h, then treated with erastin (Era, 5 μM) and the recombinant chemerin (20 ng/ml) for an additional 24 h. (**A**) Chemerin-induced ATP levels were counteracted by SLC7A11 knockdown. n = 3 (independent experiments). (**B**) The decrease in lipid peroxidation induced by chemerin was reversed by SLC7A11 knockdown. Oxidized lipids were captured using C11 BODIPY and measured by flow cytometry. n = 3 (independent experiments). (**C**) Quantified data for lipid peroxidation shown in (**B**). Data are presented as the mean ± SD. * $p < 0.05$, by one-way ANOVA with Tukey's multiple comparison test.

Supplementary Fig. 8

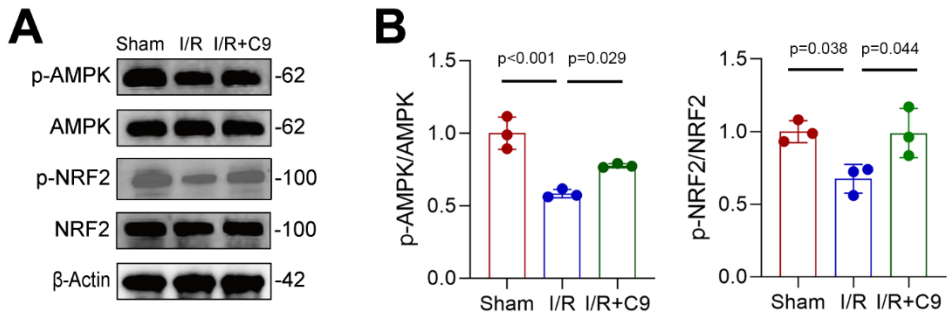

Supplementary Figure 8. C9 treatment increases p-AMPK and p-NRF2 in the kidneys of I/R model mice. (A) Protein levels of p-AMPK, AMPK, p-NRF2, and NRF2 in the kidneys of I/R model mice. Protein expression was analyzed by western blot, with b-Actin as a loading control. n = 3 (independent experiments). (B) Quantified data of western blots in (A). Data are presented as the mean ± SD. * $p < 0.05$ and *** $p < 0.001$, by one-way ANOVA with Tukey's multiple comparison test.

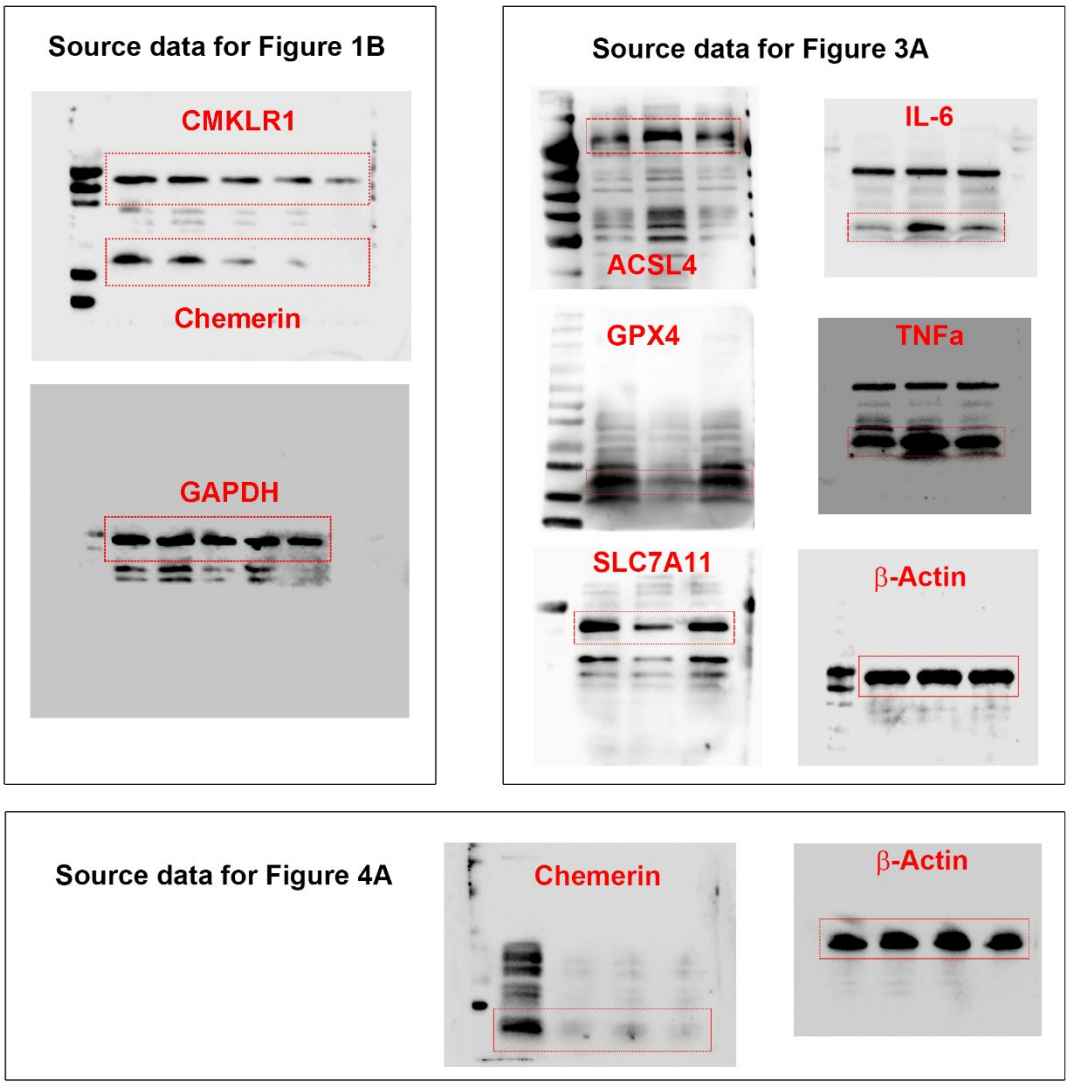

Supplementary Figure 9. Uncropped western blots.

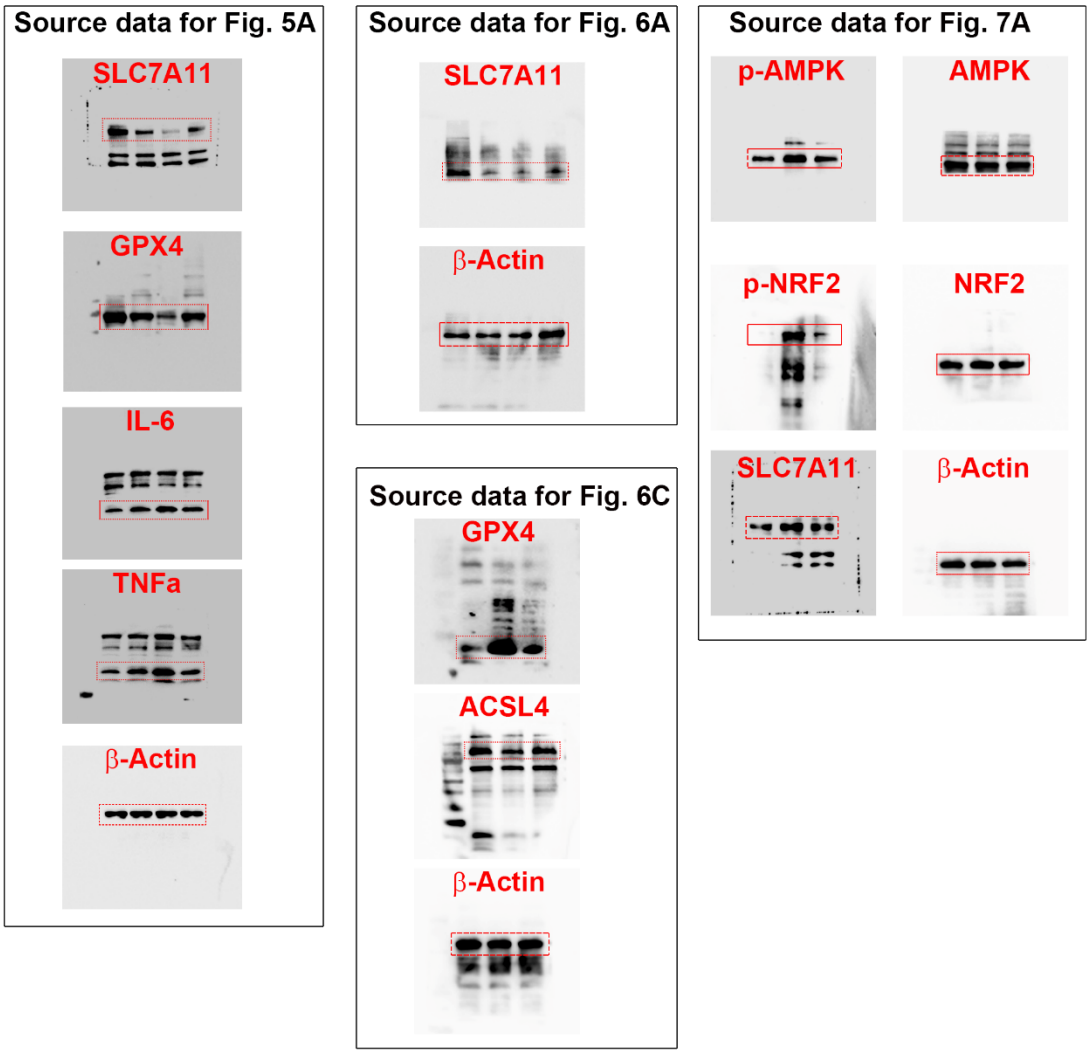

Supplementary Figure 10. Uncropped western blots.

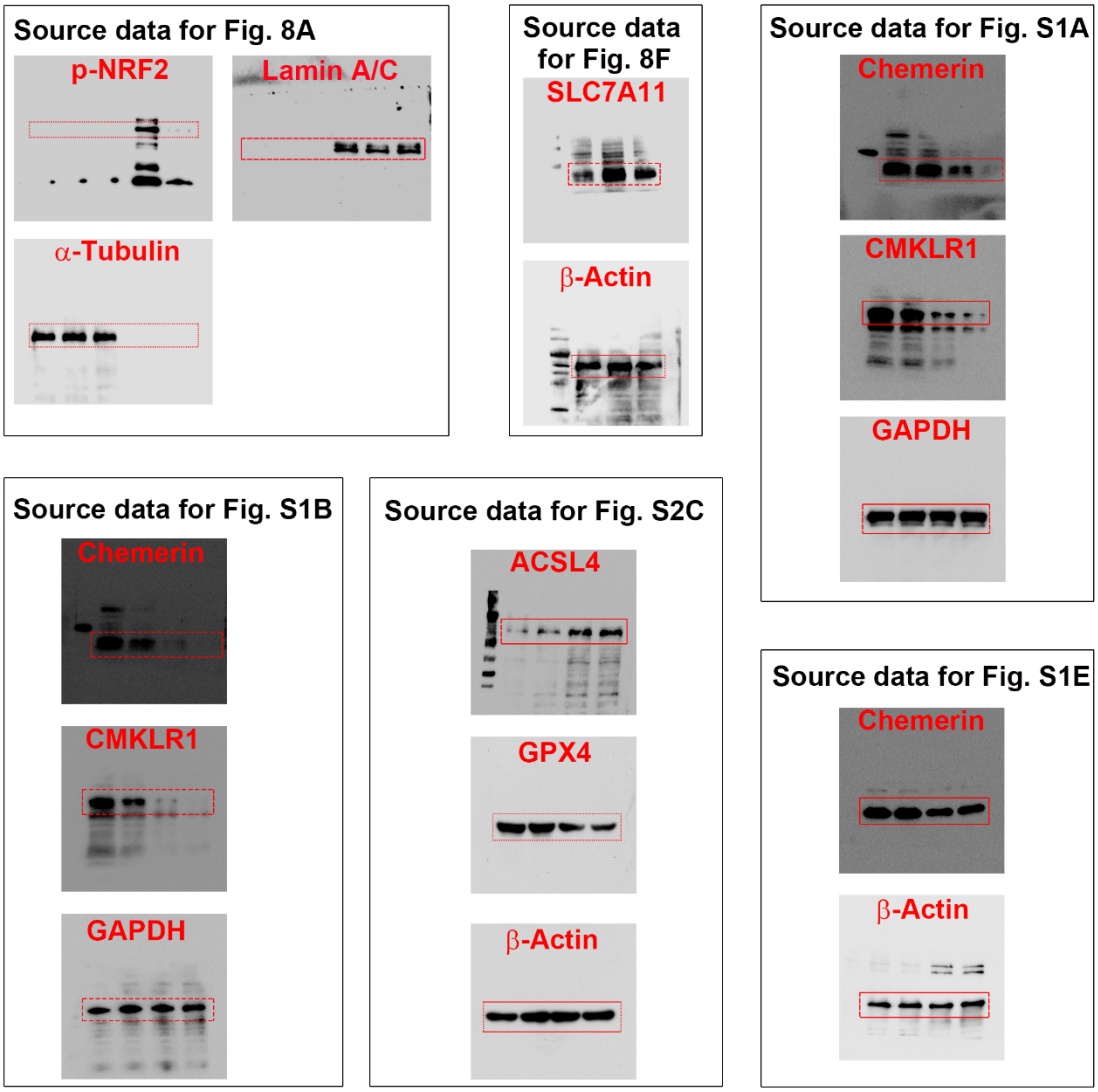

Supplementary Figure 11. Uncropped western blots.

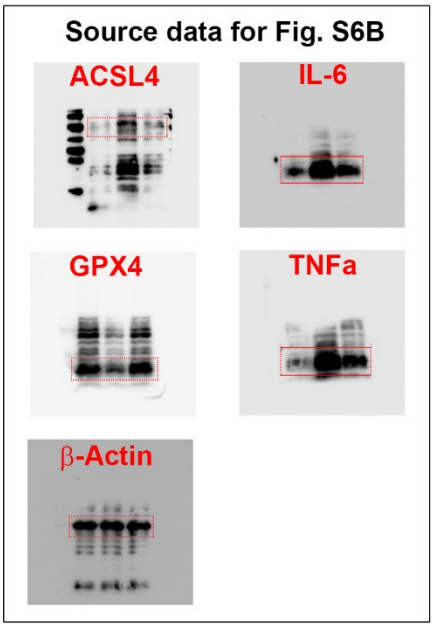

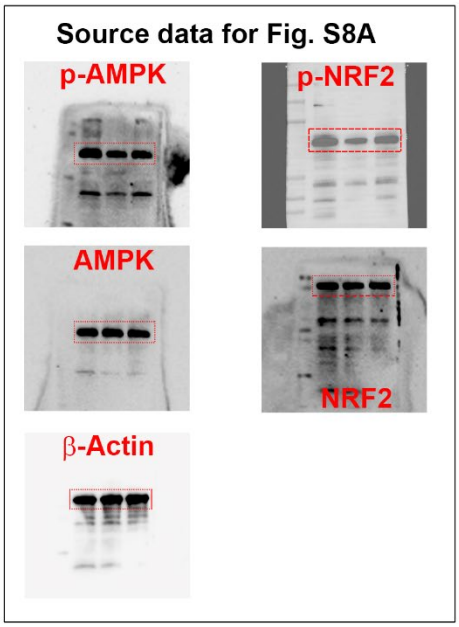

Supplementary Figure 12. Uncropped western blots.